Rodriguez-Sanchez, M. R., Sanchez-Gonzalez, A. & Santana, D. (2015). Revised receiver efficiency of molten-salt power towers. *Renewable and Sustainable Energy Reviews*, 52, pp. 1331–1339.

DOI: 10.1016/j.rser.2015.08.004

Revised receiver efficiency of molten-salt power towers

M.R. Rodriguez-Sanchez[1*], A. Sanchez-Gonzalez[1], D. Santana[1].

[1] Department of Fluids and Thermal Engineering.

Carlos III University of Madrid

Av. Universidad 30, Leganés, 28911 Madrid (Spain)

*Phone number: +34 916246034, Fax: +34916249430, e-mail: mrrsanch@ing.uc3m.es

Abstract

The demonstration power plant Solar Two was the pioneer design of a molten-salt power tower in the report "Final Test and Evaluation Results from the Solar Two Project" (Pacheco, 2002) the efficiencies of the three main subsystems: heliostats, receiver and power block were measured or estimated. The efficiency of the plant and the power block could be obtained with confidence. Whereas, the efficiencies of the heliostat field and the receiver could only be estimated because the solar flux reflected by the heliostats and intercepted by the receiver cannot be measured. The receiver efficiency was estimated using the Power-On Method. The authors themselves highlight that this method contain an important assumption: the temperature distribution on the receiver surface is independent of the incident power level. This assumption is equivalent to have a Biot number much smaller than one. For Solar Two reported data the Biot number is of order unity, and then the external tube temperature depends of the receiver load; being the thermal losses linearly with the incident solar flux rather than constant. Besides, our results show that receiver efficiency is around 77% for full load and 70% for half load instead of 87% and 80% reported assuming external tube temperature independent of the incident power.

Key words: *Solar receiver; Molten salt; Thermal efficiency; Biot number; Thermal losses.*

Nomenclature

DNI : Direct Normal Insolation.

POM : Power –On Method.

SAPS : Static Aim Processing System.

SPT : Solar Power Tower.

Symbols

Bi : Biot number. (-)

Cp : Specific heat. (J/kg °C)

H : Receiver length. (m)

L : Receiver length. (m)

L_{th} : Thermal losses. (W)

P : Power. (W)

Re : Reynolds number. (-)

T : Temperature. (°C)

d : Tube diameter. (m)

h : Convective coefficient. (W/ m^2 K)

k : Conductive coefficient. (W/m K)

$\dot{m}$: Mass flow. (kg/s)

q'' : Heat flux. (W/m^2)

v : Salt velocity. (m/s)

y : Thermal losses ratio. (-)

z : Axial coordinate. (m)

Greek letters

α : Absorptivity. (-)

ε : Emissivity. (-)

η : Thermal efficiency. (%)

ρ : Reflectivity. (-)

σ : Stefan-Boltzmann constant. (W/m^2K^4)

Subscripts

abs : Absorbed

conv : Convection.

i : Internal

inc : Incident.

o : External.

rad : Radiation.

salt : Salt.

we : External wall.

1. Introduction.

The increasing problem of CO_2 emissions has strengthened interest in renewable energy source. Solar Power Tower (SPT) is known as an important candidate for becoming in a major clean technology for commercial electricity power generation in the medium-term.

A STP is formed by three main subsystems: heliostat field, receiver and power block. The industry and laboratory research efforts are now focusing on optimizing the efficiency of the SPT. The power block is usually a traditional Rankine cycle, widely studied. Then, the global plant and the power block efficiency could be obtained with confidence because it is possible to reliably measure the input and the output data of the plant: Direct Normal Insolation (DNI), heliostats area, salt flow rate, salt temperature, and gross-electrical output.

However, the solar flux reflected by the heliostats and intercepted by the receiver cannot be measured, and then the efficiencies of the heliostat field and the receiver could only be estimated. In a SPT the receiver plays the important role of intercepting the reflected solar radiation from the heliostat field and transferring it to the heat transfer fluid. The main challenge associated with this process is the high temperature gradient at the receiver surface and transient thermal processes that may lead to local hot spots, and consequently, degradation or failure of the receiver [1]. Therefore, the receiver temperature

distribution must be carefully controlled. The temperature distribution at the receiver surface depends on the heat flux distribution, which is closely connected with the heliostat field and the aiming strategy [2].

The heliostat field layout is another key in a SPT due to its high capital investment cost (approximately 45% of the plant-total cost [3]). Then, the proper estimation of the heliostat field is an economical target. Several models predict the solar flux distribution on the receiver and the optical efficiency of the heliostat field. Walzel et al. [4] proposed a sixth order Hermite polynomial to obtain the flux map at the receiver. This model was first implemented in the RCELL code [5], then in the DELSOL [6], and most recently in the SAM software [7]. Another approximate function, based on a single circular Gaussian distribution, is used by HFLCAL code [8]. Collado et al. [9] obtained an analytical expression based on the error function, which is implemented in the UNIZAR model.

In addition, numerous authors based their studies in the thermal characterization of the molten salt receivers. Jianfeng et al. [10] implemented a theoretical model that investigated the heat transfer performance of external receivers under unilateral concentrated solar radiation, obtaining receiver performances between 87 - 92%. Singer et al. [11] made a similar study assuming no circumferential variations at the tube wall temperature, and their receiver thermal efficiency was comprised between 85-87%. Moreover, Lata et al. [12] made a sensitivity analysis of a receiver panel based on the design of the Solar Tres receiver using the SENREC code; obtaining receiver efficiencies of 77- 87%. However, since the amount of experimental data and studies concerning central receivers in the literature is reduced, the validation of these models is quite difficult.

Radosevich [13] reported the experimental test results of the demonstration power plant Solar One, a direct steam-generation plant. He estimated the receiver efficiency as the unknown in a global energy balance. Where, the efficiencies of the global power plant and the power block were calculated, and the efficiency of the heliostat field was simulated by means of MIRVAL code. The receiver thermal efficiencies obtained were comprises between 70% – 76%. In addition, Baker [14] stablished that "*the thermal losses in the Solar One receiver fit linearly with the incident power*".

Pacheco et al. [15] studied the demonstration power plant Solar Two, which was the pioneer design of a molten-salt power tower. He implemented a Power-On Method (POM) to calculate the receiver thermal efficiency. In the full knowledge that it is not entirely correct, they assumed that "*under steady-state conditions with constant inlet and outlet salt temperatures and wind velocity, the temperature*

distributions on the receiver surface and thorough the receiver are independent of the incident power level. Therefore, the thermal losses are also independent of the incident power". As a function of the solar irradiation and the wind speed, they obtained receiver performances of 80% – 87%.

The main goal of this work is to determine the receiver thermal efficiency using the data of the Solar Two Project, estimating the ratio between the thermal losses for half and full power. The POM is a good first approximation to calculate the receiver efficiency. However, it does not consider the tube wall temperature variations with the incident solar-flux distribution, and then assumes that the Biot number is lower than one. We show that in the Solar Two receiver the Biot number is of order unity, and then the estimated thermal efficiencies of the receiver are lower than those predicted by Pacheco et al. [15]. These results permit a more accurate design and a revision of the objectives to improve SPT performance.

2. Solar Two: experimental procedure

Experimental data of SPT are scarce in the literature. For SPT working with molten salt only Pacheco et al. [15] have published experimental data. Since the incident power could not be measured directly on the receiver surface [16], they designed a series of experiments carried out in the Solar Two power plant in order to calculate the efficiency of the receiver.

The experimental procedure divided the heliostat field into two groups with an equal number of heliostats symmetrically dispersed around the receiver. In this way, the power on the receiver could be halved regardless of the field cleanliness, mirror corrosion, and heliostat availability.

During 9 clear-sunny days four different tests were performed symmetrically about solar noon between 11:00 a.m. and 1:00 p.m. solar time. In the different periods of time, all the heliostats of the field (full power: cases A and C) or one half of the heliostats, scattered around the receiver (half power: cases B and D), were under operation, see Table 1 and Figure 2 for further information.

Table 1: Sequence of heliostat tracking the receiver [15].

Period	Solar Time	Heliostat Group(s)	Incident Power (Available)
A	11 a.m. to 11:30 a.m.	1 and 2	100 %
B	11:30 a.m. to 12 p.m.	1	50 %
C	12 p.m. to 12:30 p.m.	1 and 2	100 %
D	12:30 p.m. to 1 p.m.	2	50 %

In order to keep constant the outlet temperature of the salt, the mass flow rate at the receiver was adjusted for each period of time. Then, because of symmetry the average incident power during period A is twice the average incident power during period D. Likewise, for periods C and B.

After defining the experimental procedure, the averaged data collected by Pacheco et al. [15] were: the heliostat availability, the mass flow rate at the receiver, the inlet and outlet temperature of the salt, the DNI, and the wind direction and speed, see Table 2.

Table 2: Summary of key measurements during receiver efficiency tests [15].

Test Date:	29/09/97	30/09/97	01/10/97	05/03/99	12/03/99	17/03/99	22/03/99	23/03/99	24/03/99
Heliostats Tracking Receiver									
A	1767	1764	1804	1668	1685	1681	1699	1626	1725
B	883	883	897	831	853	836	847	809	858
C	1767	1758	1798	1664	1684	1676	1692	1625	1720
D	884	876	898	833	830	840	847	805	848
Average Mass Flow ($\dot{m}$) [kg/s]									
A	80	90	90	81	67	78	69	61	70
B	39	43	44	36	32	37	32	28	33
C	85	91	91	80	73	80	70	65	73
D	39	43	42	38	33	36	32	30	32
Average Inlet Temperature [ºC]	295	301	305	308	303	302	301	302	299
Average Outlet Temperature [ºC]	551	550	550	564	563	564	563	561	564
Average Ambient Temperature [ºC]	32	33	33	16	14	18	18	16	17
Average Direct Normal Insolation [W/m^2]	913	975	942	989	898	960	871	874	894
Average wind speed [m/s]	0.6	1	0.6	3	1.8	1.4	0.9	7.9	1.3
Average wind direction (Clockwise from North)	131	241	210	270	223	241	165	263	241

3. Power-On Method Analysis

The receiver efficiency is defined as the ratio of the average power absorbed by the working fluid to the average power incident on the receiver, and it is evaluated under steady-state-conditions.

$$\eta = \frac{\overline{P}_{abs}}{\overline{P}_{inc}} \qquad (1)$$

From a heat balance on the receiver during steady-state conditions, the power incident on the receiver equals the sum of power reflected by the receiver, the power absorbed by the salt, and the receiver

thermal losses (radiation, convection, and conduction), see Equation 2. The absorbed power is obtained using the inlet and outlet temperatures of the salt and the mass flow rate measured in the receiver.

$$\overline{P}_{inc} = \rho\overline{P}_{inc} + \overline{P}_{abs} + \overline{L}_{th} \qquad (2)$$

Following the Power-On Method (POM) [15], the efficiency was obtained by eliminating the incident power from the heat balance equation and by calculating the thermal losses from known measurements. In addition, to solve the problem they made the following assumption in the full knowledge that it can be taken only as a first approximation: "*Under steady-state conditions with constant inlet and outlet salt temperatures and wind velocities, the temperature distributions on the receiver surface and throughout the receiver are independent of incident power level ($T_{we,A} = T_{we,D}$). Therefore, the thermal losses are also independent of the incident power ($L_{th,A} = L_{th,D}$)*".

However, this assumption is contrary to the results obtained in a previous work [17], in which a simplified thermal model to calculate the receiver efficiency was developed. Rodríguez-Sánchez et al. [17] found that the tube wall temperature depends on the incident power and its distribution. It can be seen applying an energy analysis on the receiver. The heat flux absorbed by the molten salt at the receiver tubes can be expressed by Equation 3. Where, the heat power absorbed by the salt, the convective coefficient, the external tube wall temperature, and the mass flow rate depend on the incident power level; while the bulk temperature of the salt, the conductivity of the tube material, and the tube diameters are independent of that power.

$$P_{abs} = \left(\frac{d_o}{d_i h} + \frac{d_o \ln(d_o/d_i)}{2k} \right)^{-1} \pi d_o L \left(T_{we} - T_{salt} \right) = \dot{m} Cp \Delta T_{salt} \qquad (3)$$

Gnielinski [18] revised the heat transfer correlation for turbulent flow in tubes finding that the convective coefficient grows as the Reynolds number raised to the power between 0.75 and 0.87. For simplicity, it has been assumed that the convective coefficient is proportional to the Reynolds number, and then to the salt velocity ($h \propto \mathrm{Re} \propto v$). Equations 4 results from Equation 3, where the Biot number is defined as the ratio between conduction and convection resistances, $Bi = h d_i \ln(d_o/d_i)/2k$.

$$P_{abs} = \pi L d_i h \left(1 + Bi\right)^{-1} \left(T_{we} - T_{salt} \right) = \dot{m} Cp \Delta T_{salt} \qquad (4)$$

Equation 5 is obtained dividing a percentage of the full absorbed power (P'_{abs}) by the full absorbed power. Where it has been assumed that the convective coefficient and the mas flow rate vary proportionally to the salt velocity, and then $h\dot{m}'/(h'\dot{m}) \simeq 1$.

$$\frac{(1+Bi')}{(1+Bi)} = \frac{(T'_{we} - T_{salt})}{(T_{we} - T_{salt})} \qquad (5)$$

It can be noticed that the only condition to match the tube wall temperature for a full power or any lower power is that the Biot number tends to zero. That means that the resistance by conduction must be negligible with respect to the resistance by convection. To fulfil that condition it is necessary that at least one of the following assumptions be achieved:

- Extremely high conductivity of the tube material. Nevertheless, the Solar Two tubes are 316 stainless steel, whose conductivity coefficient is $k \simeq 20 W/\text{m}^{\text{o}}\text{C}$.
- Slim tubes (1.2 mm for Solar Two), however thickness reduction is limited because it is detrimental for the mechanical behaviour of the tubes, generating a reduction of the receiver operational life.
- Small tube diameter (21 mm for Solar Two), but it increases the pressure drop and the consumption of the feed pumps [17]. In addition, a reduction of the tube diameter produces an increment of the salt velocity and of the convective coefficient, being contrary to the Biot number decrement.
- High circumferential diffusion in the tube surface, but in a previous work [17] it has been demonstrated that the circumferential diffusion is negligible respect to the radial one.

For the Solar Two reported data the tube wall conduction and the internal convection resistances are of the same order. Therefore, the Bi number must be taken into account to calculate the receiver thermal efficiencies and the tube wall temperature, which would be higher for full power than for half power. Figure 1 represents the Biot number as a function of the absorbed power for September 29th 1997 reported by [15]. It can be seen that in this kind of problems the Biot number is not constant, it increases with the absorbed power in a nonlinear way, neither negligible, for an absorbed power of 100% de Biot number is 2.8.

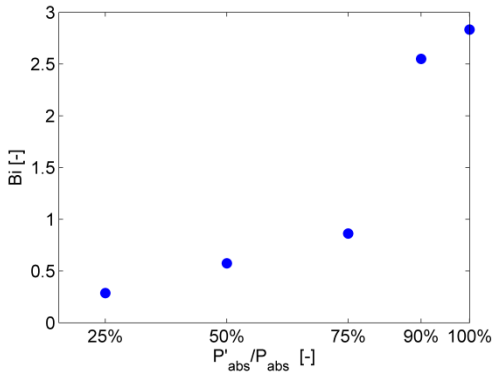

Figure 1: Variation of the Biot number as a function of the absorbed power.

Once it has been proved the necessity of considering the Biot number in this problem, a modification in the Power-On Method has been introduced, in order to take into account the heat losses variations with the incident power. The differences between the thermal losses for full and half power have been included as $L_{th,\mathrm{D}} = yL_{th,\mathrm{A}}$. Then, under this assumption, the equations used by POM to obtain the thermal losses and the receiver efficiency are the following ones:

$$\begin{cases} P_{inc,A} = 2P_{inc,D} \\ P_{inc,C} = 2P_{inc,B} \end{cases} \Rightarrow \begin{cases} P_{abs,\mathrm{A}} + L_{th,A} = 2P_{abs,D} + 2yL_{th,A} \\ P_{abs,C} + L_{th,C} = 2P_{abs,B} + 2yL_{th,C} \end{cases} \tag{6}$$

$$L_{th,A} = L_{th,\mathrm{C}} = \frac{\left(P_{abs,A} + P_{abs,C} - 2P_{abs,B} - 2P_{abs,D}\right)}{4y - 2} \tag{7}$$

$$L_{th,\mathrm{D}} = L_{th,\mathrm{B}} = yL_{th,A} = yL_{th,C} \tag{8}$$

$$\eta = \frac{P_{abs}}{P_{inc}} = \frac{\alpha}{1 + \frac{L_{th}}{P_{abs}}} \tag{9}$$

Pacheco et al. [15] assumed that the thermal losses are constant with the incident power level, $y = 1$. It has been demonstrated that this value must be lower than the unit; however it cannot be estimated using only the measured data from Solar Two and the Power-On Method. Then, a more detailed thermal model has been used to calculate the thermal losses.

3.1. Simplified thermal model.

A simplified model of the central receivers has been yet presented by Rodríguez-Sánchez et al. [17]. That model has been modified in order to adapt it as much as possible to the Solar Two operational and geometrical characteristics. In addition, it has been combined with Sánchez-Gonzalez and Santana heliostat model [19] that allows to calculate the solar flux distribution on the receiver.

The Solar Two collector field consists of 1818 heliostats (mirror area: 39.13 m^2) of the former Solar One plant and 108 new heliostats (95 m^2) added to the south side. Each heliostat coordinate has been gathered from [15]. Besides the heliostat field layout, other optical parameters have been taken from the same reference, e.g.: reflectivity, cleanliness, tracking error or heliostat availability.

Heliostats were aimed at different positions along the vertical of the receiver surface. Every 10 minutes, each heliostat aiming was commanded by the Static Aim Processing System (SAPS), which ensures a rather uniform flux distribution in the central region of the receiver. In the absence of specific aim-point information, a previously reported multi-aiming strategy [19] has been applied in the computational model. An aiming factor equal to 2.5 has been assigned in order to reduce spillage losses.

For each selected day and instant of time in the middle of each period (Table 2), the flux density distribution on the receiver has been computed using the optical model [19]. The optical efficiency at Solar Two heliostat field is represented in Figure 2 for each period during experiments of September 29th, 1997. In addition, for these experiments the measured field efficiency, ignoring heliostats reflectivity and cleanliness, was between 66% and 62%, in agreement with our model outputs (65.3%-64.7%). On the basis of the optical model, flux maps for each test period are generated, providing the necessary input for the proposed receiver thermal model [17].

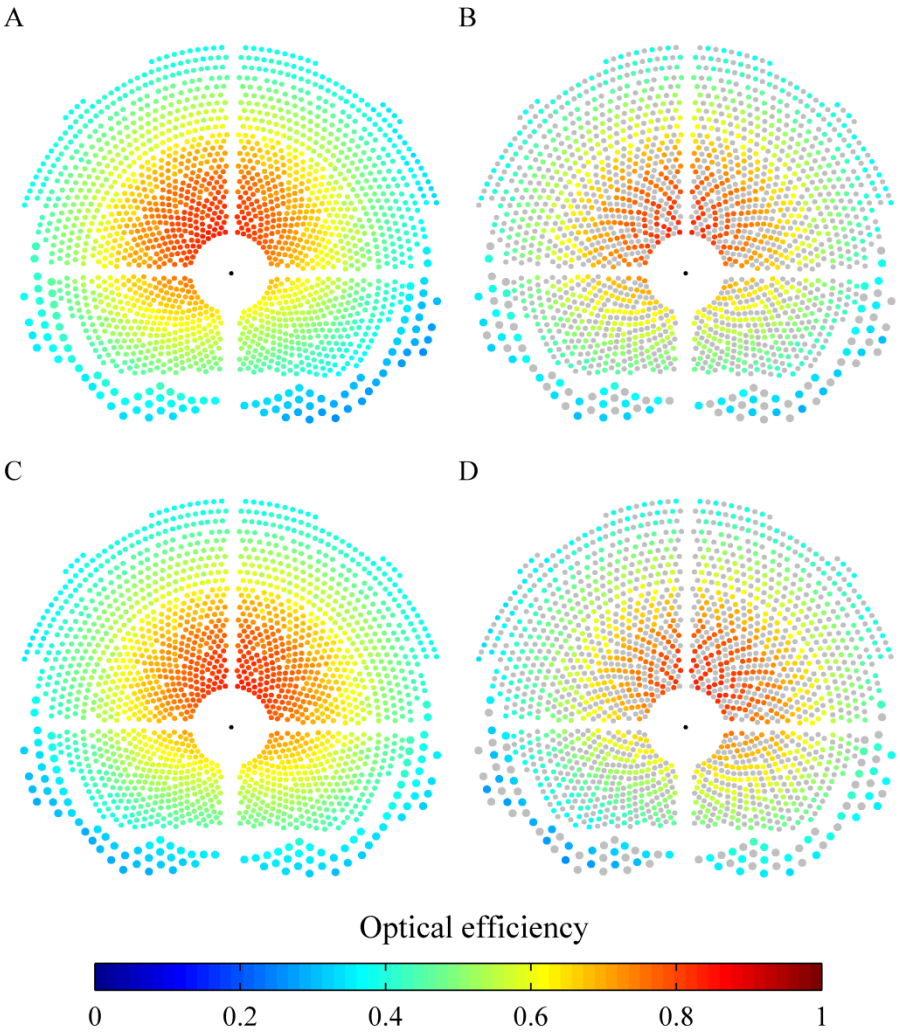

Figure 2: Simulated optical efficiency of the heliostats at Solar Two field during the four cases of September 29th, 1997.

Regarding the external receiver the main design parameters can be seen in Table 3. Although the operation mode of Solar Two have been widely described in [15], there are some unknown parameters that have to be assumed in the thermal model. To estimate the mass flow rate in the receiver, it has been imposed that the salt temperature at the outlet of the receiver for each period is that reported by [15]. By means of a valve the mass flow rate in each flow path is fitting, to fulfil the outlet temperature of the salt. Besides, the mass flow by all the tubes of a panel is assumed to be the same.

The mass flow rate predicted by the authors is slightly lower than that measured in the tests (~10kg/s), it could be associated to a difference in the solar flux distribution on the receiver. Besides, it is necessary to take into account that: the reported experimental results corresponds to averaged data over half an hour (i.e. non-instantaneous), the internal Nusselt correlation adopted in the simulations is subject to an error,

conditions of cleanliness and constant absorptivity has been assumed, the aiming point strategy for the heliostat at Solar Two is not fully described, the process of heat exchange in the head of the panels has been neglected in the thermal model, and then fully developed flow has been assumed in the whole receiver , etc.

Table 3. Main design parameters of the Solar Two heliostat field and solar receiver.

Number of Heliostat	1926
Heat Transfer Fluid	Molten Salt
Tube material	316H Stainless Steel
Receiver Diameter/ Height	5.1/ 6.2 m
Inlet/ Outlet temperature	290/ 565 ºC
Number of flow circuits	2
Number of panels	24
Number of tubes per panel	32
Tube diameter/ thickness	21/ 1.2 mm
Absorptivity	0.95 (Black Pyromark)

According to this model the thermal losses for half power are around 64% of the thermal losses for full power, $y = 0.638$.

4. Results

In this section the thermal losses and the thermal efficiency of the receiver for full and half power have been shown. They have been obtained by the Power-On Method using $y = 1$ (assumed by Pacheco et al. [15]) and $y = 0.638$ (estimated using Rodríguez-Sánchez et al. [17] and Sánchez-Gonzalez et al. models [19]).

In addition, the distribution of the tube wall temperature have been calculated and compared for both assumptions. In contrast to $y = 1$, for $y = 0.638$ differences can be seen in the tube wall temperature distribution caused by the variation of the incident power in the receiver. It produces different thermal losses for full and half power.

Figure 3 shows the thermal losses and the receiver thermal efficiency obtained by the POM and $y = 1$, assuming that the thermal losses are equal for full and half power. In addition, it can be seen the results obtained for the POM and $y = 0.638$. In this way, the thermal losses are dependent of the incident power and in both cases are higher than the thermal losses predicted with $y = 1$. It is due to the elevated wall temperature in the front part of the tubes (see Figure 4). Since the thermal losses are higher, the receiver

efficiencies are lower than those expected by y =1, approximately a 10% lower. In addition, the averaged values for all the test days of each experiment are shown.

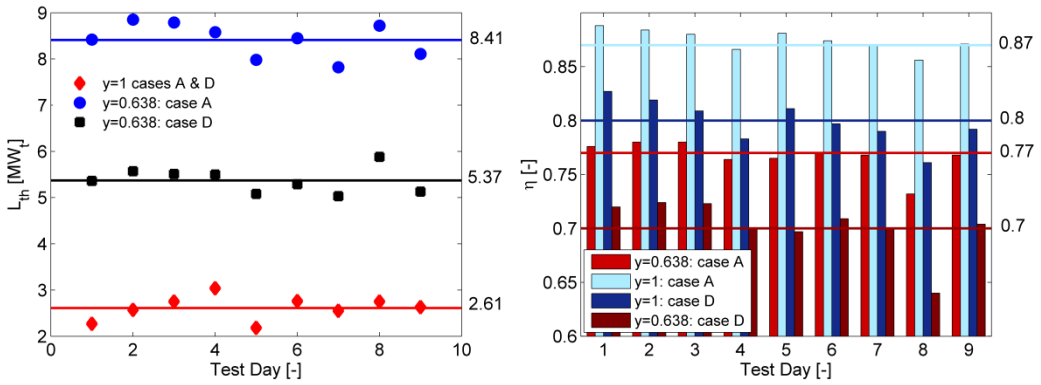

Figure 3. a)Thermal losses and b) Receiver efficiency comparison for case A and D using y =1 and y =0.638.

The estimated y =0.638 generates different heat losses for full and half power. And as it was expected the heat losses for full power are higher than for half power (see Figure 3.a). In addition, the heat losses obtained with this y are for both cases higher that the predicted by the assumption of y =1. The maximum difference in the thermal losses between both y values is 7.8MW for the full field during March 5th 1999. This day the differences are maximum due to the molten salt enters to the receiver at the highest temperature, 308 ºC, compared to September 29th 1997 when the salt enters at 295 ºC. A difference of 13 ºC in the molten salt, reduces its capacity of absorb heat, affecting to the wall temperature and then to the thermal losses.

Considering that the receiver temperature distribution is dependent on the incident power (y =0.638) the thermal efficiency decreases in average a 10% respect to the y =1 (see Figure 3.b). The maximum efficiency difference is 17.4% for the 23th of March, a day with high wind speed, low DNI and low mass flow rate in the receiver.

Taking into account the whole plant, the global efficiency must be 15% [15]. For y =0.638 multiplying the three efficiencies: power block (34% calculated in [15]), heliostat field (57%) and receiver (77%) the expected global efficiency has been obtained. However, for y =1 the global efficiency is slightly higher, attributed to a mistake in the heliostat field model [15].

Figure 4 represents the temperature distribution in every panel of the receiver according to the thermal model (y =0.638) for September 29th 1997. It can be seen how the surface temperature distribution varies with the incident power. Figure 4.a corresponds to full power distribution (case A), circumferential variations of the tube wall temperature can be observed. The maximum tube wall temperature reaches 639.8 ºC in the external part of the tubes sited on the west/east side of the receiver. Figure 4.b depicts the tube wall temperature distribution of the receiver working at half power (case D), its maximum value is 587.7 ºC, and it is found in the same location than for case A.

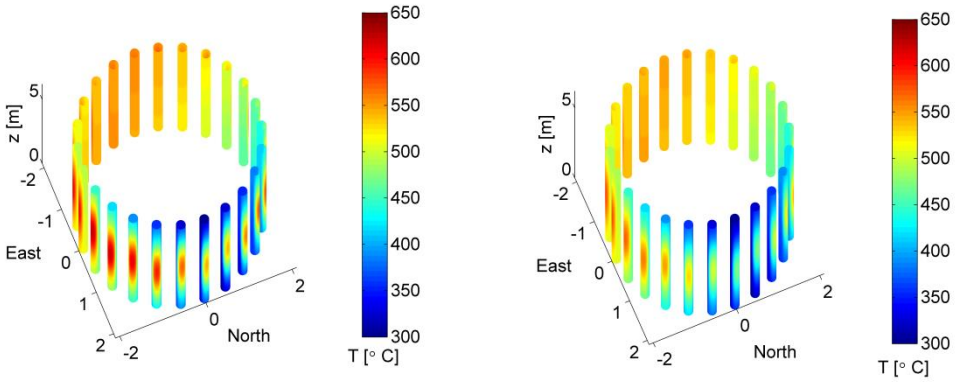

Figure 4: Tube wall temperature distribution using y =0.638 for September 29th 1997. (a) Case A. (b) Case D.

Figure 5 shows the temperature distribution of the receiver tubes as the result of applying the hypothesis of y =1 ([15]). The first problem found was that it is impossible to fix the three dependent variables: incident power, mass flow rate and outlet salt temperature. Then, it was decided to keep constant the absorbed power varying the incident one. The day shown is September 29th 1997 and case A, although according to Pacheco et al. [15] the case is indifferent because all them have the same temperature distribution. As has been previously shown the tube wall temperature does not vary circumferentially. In this case the maximum tube wall temperature is 569 ºC and it is located in the southern tubes. It means that modifying the y value the tube wall temperatures differ in 70 ºC. It has strong influence in the heat losses, mainly in the radiative heat losses.

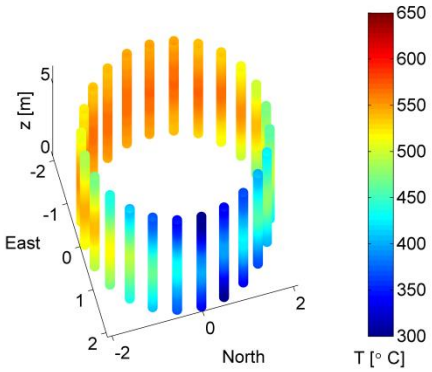

Figure 5: Tube wall temperature distribution using y =1 for September 29th 1997.

It is not the same the average temperature at the fourth potency than the individual temperature at the fourth potency averaged ($\overline{T^4} > \overline{T}^4$). Then, the effective temperature of radiation calculated with y =0.638 for full and half power of September 29th 1997 is 794 ºC and 772 ºC, respectively. While for y =1 the value of this temperature is 636.6 ºC, calculated by Equation 4 and full power. The difference in the effective temperature of radiation affect to the thermal losses and then to the thermal efficiency, as can be seen in Figure 3.

4.1. Variation of the incident thermal power.

In this subsection we have extended the Solar Two results for half and full power reported by Pacheco et al. [15] to different incident power of the receiver by means of the thermal model developed by the authors.

Figure 6 shows the tube wall temperature distribution along the receiver and how it varies as a function of the incident power (25%, 50%, 75% and 100%) from the day September 30th 1997. In addition, it can be seen the average salt temperature evolution, that is practically constant for the fourth incident power analysed.

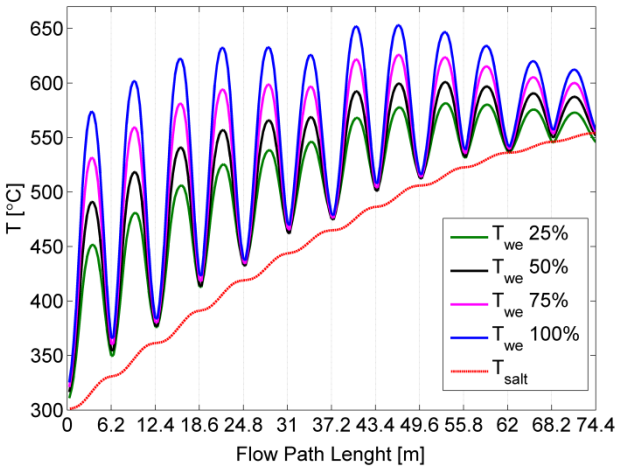

Figure 6. Tube wall temperature distribution along the receiver as a function of the incident power

In Figure 6 it is shown that the tube wall temperature is strongly affected by the incident power, moreover in the centre of the tubes. The maximum tube wall temperature is 653 ºC for the maximum incident power, for a 75% of this power the maximum wall temperature decreases to 626 ºC, while for a 25% decreases to 582 ºC. These 71 ºC respect to the total incident power could have a fatal influence in the mechanical behaviour of the tubes and in their life time operation.

Figure 7.a presents the relative heat losses as a function of the incident power. It can be noticed that the thermal losses ratio is lineal with respect the incident power, in this way it can be said that for the Solar Two the thermal losses ratio, y , can be expressed as a lineal function of the incident power, see Equation 10. In addition, it is observed that for an incident power of 25% the thermal losses are reduced 60% respect to the full load case.

$$\frac{L'_{th}}{L_{th}} = y = 0.8\frac{P'_{inc}}{P_{inc}} + 0.22 \qquad (10)$$

Figure 7.b shows the receiver thermal efficiency relation as a function of the incident power. It can be seen that the efficiency increases with the incident power even though the thermal losses increases too. The receiver efficiency varies smoother than the thermal losses, less than 20% when the incident power is a 25%; and this variation is not linear. Although the receiver efficiency increases with the incident power, and then with the thermal losses, it is always lower than the estimated by the Power-On Method for $y = 1$.

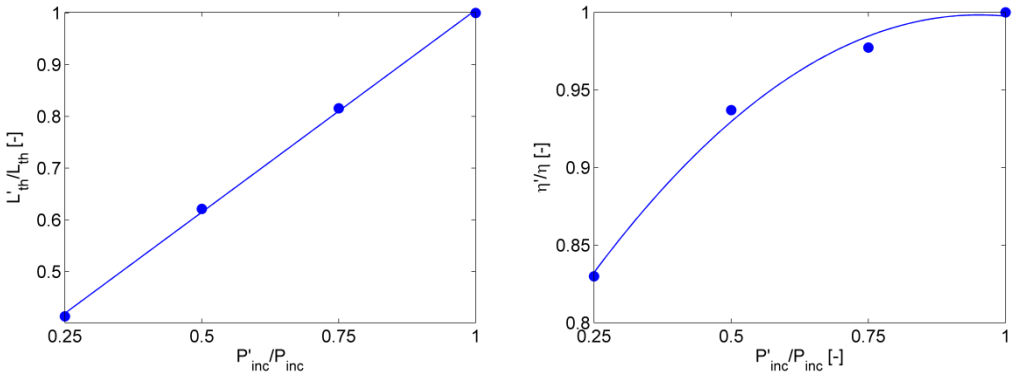

Figure 7. a) Thermal losses ratio and b) receiver thermal efficiency ratio as a function of the incident power for Solar Two project.

Then, given the y expression, and measuring the absorbed power for any ratio of incident power it is possible to calculate, by means of the Power-On Method, any thermal behaviour of the receiver using the following equations. However, when y is missing another model more detailed it is necessary to calculate these values, due to the thermal losses varies with the incident power.

$$L_{th} = \frac{P'_{abs} - P_{abs}\dfrac{P'_{inc}}{P_{inc}}}{0.2\dfrac{P'_{inc}}{P_{inc}} - 0.22} \quad (11)$$

$$\eta = \frac{P_{abs}}{P_{inc}} = \frac{\alpha P_{abs}}{P_{abs} - L_{th}} \quad (12)$$

Figure 8 is the result of applied the Equations 11 and 12 for Solar Two receiver. As it was said before, it has been obtained that for full power the heat losses are 9 MW and the receiver efficiency of 0.78 for full power. Moreover, the values of these variables for 25% and 75% of power can be obtained without the necessity of experimental measures.

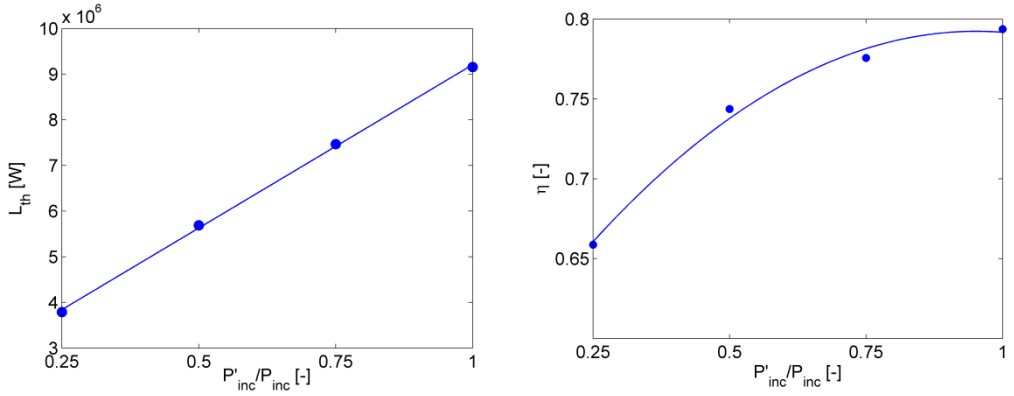

Figure 8. a) Thermal losses and b) receiver thermal efficiency as a function of the incident power for Solar Two project.

5. Conclusions

The precise estimation of the thermal behaviour of the central receiver of a SPT is necessary to avoid damages in this system. Furthermore, it is important for the design of the heliostat field, the most expensive part of a SPT. An oversized heliostat field means an unnecessary investment cost, while and undersized heliostat field reduces the electrical energy production of the SPT.

To calculate the receiver efficiency Pacheco developed the Power-On Method [15] on the basis of the experimental test results of the pilot plant Solar Two. In that model the following assumption, in the full knowledge that it is not entirely correct was made: *Under steady-state conditions with constant inlet and outlet salt temperatures and wind velocities, the temperature distributions on the receiver surface and throughout the receiver are independent of incident power level ($T = T_{1/2}$). Therefore, the thermal losses are also independent of the incident power ($L_{th} = L_{th,1/2}$).* It is the same that neglect the conductivity of the receiver tubes and considers the Bi number much lower than one. However, from Solar Two reported data it can be calculated that the tube wall conduction and the internal convection resistances are of the same order ($Bi = 2.8$), and then the Bi number must be taken into account to obtain the receiver thermal efficiencies, and the tube wall temperature.

Therefore, the Power-On Method cannot be employed while the thermal losses ratio or at least the thermal losses for full power are not measured. In the absence of more detailed experimental data the authors have used a previous developed thermal model for central receivers [17,19]. In this way, a lineal relation between the thermal losses and the incident power has been found $L'_{th}/L_{th} = y = 0.8\,P'_{inc}/P_{inc} + 0.22$. The thermal losses for half power are 63.8% of the thermal losses for full power. This thermal losses relation allows to extend the model for any ratio of incident power, even in absence of experimental data of a particular incident power.

In addition, the thermal model allows to calculate the tube wall temperature distribution as a function of the incident power. In a receiver tube there are circumferential variations of the surface temperature that modify the effective temperature of radiation from 640 ºC for $y = 1$ to 800 ºC for $y = 0.638$. According to POM with $y = 1$, in which there are not circumferential variations, the thermal losses of the receiver were 2.61 MW. However, for the POM with $y = 0.638$, in which these variations are taken into account, the thermal losses increase up to 9.33 MW for the full field. As a consequence, the thermal efficiency of the

receiver decreases a 10%, from 87% to 77%; it is agreement to the global plant efficiency. These results would permit a more accurate design and a revision of the objectives to improve SPT performance.

Acknowledgements

The authors would like to thank the financial support of the Spanish government for the project ENE2012-34255.

Bibliography

[1] Winter CJ, Sizmann RL, L V-HL. Solar Power Plants. Berlin, Heidelberg: Springer Berlin Heidelberg; 1991.

[2] Salomé A, Chhel F, Flamant G, Ferrière A, Thiery F. Control of the flux distribution on a solar tower receiver using an optimized aiming point strategy: Application to THEMIS solar tower. Sol Energy 2013;94:352–66.

[3] Collado FJ. Quick evaluation of the annual heliostat field efficiency. Sol Energy 2008;82:379–84.

[4] Walzel MD, Lipps FW, Vant-Hull LL. A solar flux density calculation for a solar tower concentrator using a two-dimensional hermite function expansion. Sol Energy 1977;19:239–53.

[5] Lipps FW, Vant-Hull LL. A cellwise method for the optimization of large central receiver systems. Sol Energy 1978;20:505–16.

[6] Kistler BL. A User's Manual for DELSOL3: A Computer Code for Calculating the Optical Performance and Optimal System Design for Solar Thermal Central Receiver Plants. Alburquerque: 1986.

[7] Golden C. System Advisor Model. Natl Renew Energy Lab 2013:sam.nrel.gov/content/downloads, 19–09–2014.

[8] Schwarzbözl P, Pitz-Paal R, Schmitz M. Visual HFLCAL - A Software Tool for Layout and Optimisation of Heliostat Fields. SolarPACES, 2009.

[9] Collado FJ, Gómez A, Turégano JA. An analytic function for the flux density due to sunlight reflected from a heliostat.pdf. Sol Energy 1986;37:215–34.

[10] Jianfeng L, Jing D, Jianping Y. Heat transfer performance of an external receiver pipe under unilateral concentrated solar radiation. Sol Energy 2010;84:1879–87.

[11] Singer C, Buck R, Pitz-Paal R, Müller-Steinhagen H. Assessment of Solar Power Tower Driven Ultrasupercritical Steam Cycles Applying Tubular Central Receivers With Varied Heat Transfer Media. J Sol Energy Eng 2010;132:041010: 1–12.

[12] Lata JM, Rodrí uez M, de Lara MA. High Flux Central Receivers of Molten Salts for the New Generation of Commercial Stand-Alone Solar Power Plants. J Sol Energy Eng 2008;130:021002:1–5.

[13] Radosevich LG. Final Report on the Power Production Phase of the 10MWe Solar Thermal Central Receiver Pilot Plant. Livermore, California: 1988.

[14] Baker AF. Techniques for Processing Experimental Data From a Solar Central Receiver to Evaluate the. J Sol Energy Eng 1990;112:6–11.

[15] Pacheco JE. Final Test and Evaluation Results from the Solar Two Project. Alburquerque, SAND2002-0120: 2002.

[16] Pacheco JE, Houser RM, Neumann A. Concepts to measure flux and temperature for external central receivers.pdf. Jt. Sol. Eng. Conf., 1994, p. 595–603.

[17] Rodríguez-Sánchez MR, Soria-Verdugo A, Almendros-Ibáñez JA, Acosta-Iborra A, Santana D. Thermal design guidelines of solar power towers. Appl Therm Eng 2014;63:428–38.

[18] Gnielinski V. On heat transfer in tubes. Int J Heat Mass Transf 2013;63:134–40.

[19] Sánchez-González A, Santana D. Solar flux distribution on central receivers: a projection method from analytic function. Renew Energy 2015;74:576–87.